Carcinogenesis, 2023, **44**, 871–883
https://doi.org/10.1093/carcin/bgad073
Advance access publication 16 October 2023
Original Article

Original Article

Lnc-PKNOX1-1 inhibits tumor progression in cutaneous malignant melanoma by regulating NF-κB/IL-8 axis

Anlan Hong[1], Meng Cao[1], Dongqing Li[1], Yixin Wang[1], Guoqiang Zhang[2], Fang Fang[1], Liang Zhao[1], Qiang Wang[1], Tong Lin[1,*] and Yan Wang[1,*]

[1]Hospital for Skin Diseases, Institute of Dermatology, Chinese Academy of Medical Sciences and Peking Union Medical College, Nanjing, China
[2]Department of Dermatology, the First Hospital of Hebei Medical University, Shijiazhuang, China

[*]Corresponding author: Tel: +86 13851897979. Email: drwangyan@163.com
Correspondence may also be addressed to Tong Lin. Tel: +86 13951902258. Email: ddlin@hotmail.com

Abstract

Cutaneous malignant melanoma is one of the most lethal cutaneous malignancies. Accumulating evidence has demonstrated the potential influence of long non-coding RNAs (lncRNAs) in biological behaviors of melanoma. Herein, we reported a novel lncRNA, lnc-PKNOX1-1 and systematically studied its functions and possible molecular mechanisms in melanoma. Reverse transcription-quantitative PCR assay showed that lnc-PKNOX1-1 was significantly decreased in melanoma cells and tissues. Low lnc-PKNOX1-1 expression was significantly correlated with invasive pathological type and Breslow thickness of melanoma. *In vitro* and *in vivo* experiments showed lnc-PKNOX1-1 dramatically inhibited melanoma cell proliferation, migration and invasion. Mechanically, protein microarray analysis suggested that interleukin-8 (IL-8) was negatively regulated by lnc-PKNOX1-1 in melanoma, which was confirmed by western blot and ELISA. Western blot analysis also showed that lnc-PKNOX1-1 could promote p65 phosphorylation at Ser536 in melanoma. Subsequent rescue assays proved IL-8 overexpression could partly reverse the tumor-suppressing function of lnc-PKNOX1-1 overexpression in melanoma cells, indicating that lnc-PKNOX1-1 suppressed the development of melanoma by regulating IL-8. Taken together, our study demonstrated the tumor-suppressing ability of lnc-PKNOX1-1 in melanoma, suggesting its potential as a novel diagnostic biomarker and therapeutic target for melanoma.

Graphical Abstract

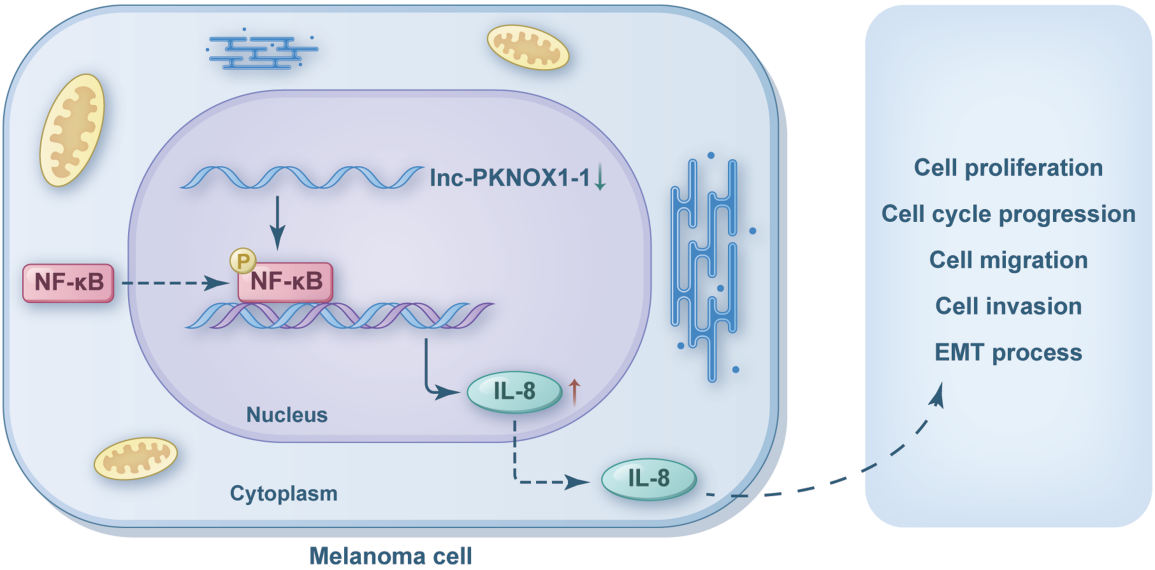

Abbreviations: CCK-8, Cell Counting Kit-8; CDK2, cyclin-dependent kinase 2; CMM, cutaneous malignant melanoma; DEGs, differentially expressed genes; EdU, ethynyldeoxyuridine; EMT, epithelial–mesenchymal transition; FISH, fluorescent in situ hybridization; IL-8, interleukin-8; lncRNAs, long non-coding RNAs; NF-κB, nuclear factor-kappa B; RACE, rapid amplification of cDNA ends; RT-qPCR, reverse transcription-quantitative PCR.

Received: June 20, 2023; Revised: September 28 2023; Accepted: October 15, 2023

Introduction

Cutaneous malignant melanoma (CMM) is one of the most lethal cutaneous malignancies and accounts for >75% of skin cancer-related deaths. It has a 5-year survival rate of 23% in late-stage melanoma patients (1). Over the past decade, the overall incidence of CMM in the USA has been reported to increase by an average of 1.4% annually (2).

Once CMM has spread, it becomes life-threatening rapidly, and it responds poorly to conventional chemotherapy and radiotherapy. In recent decades, immunotherapy and molecularly targeted therapy have progressed in treating advanced melanoma, and the overall death rate has been declining accordingly. However, both primary and acquired drug resistances are common in melanoma immunotherapy and targeted therapy. Genetic changes in melanoma differ among different ethnic groups. The decline of mortality rate is the most significant in whites, but not obvious in non-white populations (2,3). As for patients who were initially sensitive to the existing targeted and immune therapies, melanoma also tends to resist these therapies subsequently (4,5). Therefore, exploring novel molecular targets associated with melanoma progression is necessary and urgently needed.

Long non-coding RNAs (lncRNAs) are transcripts longer than 200 nucleotides and without protein-coding potential. LncRNAs can regulate multiple cellular functions, and their aberrant expression has been proved associated with a variety of human diseases, including cancer (6). It has been widely reported that lncRNAs regulate cell proliferation, metastasis, invasion, apoptosis, angiogenesis, microenvironment modification and other biological behaviors in skin cancers (6). Among them, the effects of lncRNAs in melanoma are well researched. A growing number of studies have proved the indispensable roles of lncRNAs as oncogenes or tumor suppressors in melanoma (7,8). For instance, BANCR, HOTAIR and MALAT1, which are lncRNAs highly expressed in melanoma, promote migration and invasion of melanoma; while GAS5, CPS1-IT1 and TINCR, which are melanoma-suppressing lncRNAs, inhibit proliferation, invasion and migration of melanoma (9–14).

LncRNAs can be detected in multiple body fluids, such as blood, plasma or urine. Several lncRNAs have been found in the body fluids of melanoma patients (15). For instance, high levels of lncRNA HOTAIR, SPRY4-IT1 and PVT1 have been detected in the plasma of melanoma patients, and closely related to melanoma tumor stage (16,17). Therefore, lncRNAs are promising as biomarkers for diagnosis or prognostic evaluation. Given the cancer-specific expression and multiple functional mechanisms of many lncRNAs, their development as targets for new drugs also held great promise (15).

Our previous research revealed that THOC2 functions as an oncogene in melanoma (18). We found that lnc-PKNOX1-1 was significantly downregulated after THOC2 knockdown. This study aimed to explore the clinical relevance and molecular function of lnc-PKNOX1-1 in melanoma, and to assess its potential role in melanoma prognostic evaluation and treatment.

Materials and methods

Cell culture and transfection

Normal human primary melanocytes were isolated from fresh human foreskin specimens after circumcision in our hospital, and cultured in melanocyte medium (MelM; Sciencell, USA). A375, A2058 and SK-MEL-28 cell lines were purchased from Cellcook Biotech Co., Ltd (Guangzhou, China) in September, 2020. A875 and MV3 cell lines were provided by Prof. Xiulian Xu from our institute in September 2020. HMY-1 cell line was provided by Prof. Yan Kong from Peking University Cancer Hospital and Institute in February 2021. Melanoma cell lines were cultured in Dulbecco's modified Eagle's medium with 10% fetal bovine serum (VivaCell Biosciences, China). All cells were maintained at 37°C, 5% CO_2, humidified environment. All cell lines were authenticated by short tandem repeat profiling, and the last authentication was in September 2021. Mycoplasma contamination testing was regularly conducted in all cells, and no mycoplasma contamination was confirmed.

Lnc-PKNOX1-1-overexpressed cell model was established in A375 and A2058 cells by lentivirus-mediated transfection. The lentiviral pCDH-MSCV-MCS-EF1-GFP-puro-lnc-PKNOX1-1 vector, known as OE-PKNOX1-1, and the control vector (pCDH-MSCV-MCS-EF1-GFP-puro) were purchased from IBSBio (China). The stable cell lines were selected by 1 μg/ml puromycin (Amresco, USA), and the overexpression efficiency of lnc-PKNOX1-1 was assessed by reverse transcription-quantitative PCR (RT-qPCR).

Recombinant human IL-8 protein (Proteintech, China) powder was dissolved in phosphate-buffered saline to achieve the storage solution of 0.1 mg/ml, and stored in aliquots at −20°C. Before use, the storage solution was diluted in cultured medium to 10 ng/ml, which was determined based on previous literature (19–21) and pilot experiments. For rescue assays, the cells were pretreated in medium either with interleukin-8 (IL-8) (10 ng/ml) as IL-8 overexpressing group or with an equal volume of phosphate-buffered saline as the control group, at 37°C for 24 h.

Patients and tissue specimens

This study was approved by the Ethics Committee of Institute of Dermatology, Chinese Academy of Medical Sciences. Forty pairs of melanoma tissues and adjacent normal tissues were collected from surgical patients in our hospital from September 2017 to January 2019. The diagnosis of these tissues was confirmed by pathological examination. All the patients enrolled did not receive any preoperative cancer treatments, and their written informed consents were obtained. The clinicopathological information of the patients is displayed in Table 1.

Rapid amplification of cDNA ends assay

The function of rapid amplification of cDNA ends (RACE) assay is to acquire full-length cDNA through rapid amplification of cDNA fragments with its 5′ and 3′ ends from low-abundance transcripts. RNA samples were extracted from A2058 cells. 5′ and 3′-RACE experiment was performed using GeneRacer Kit (Thermo Fisher Scientific, USA). The information on primers used for 5′ and 3′-RACE is presented in Supplementary Table 1, available at *Carcinogenesis* Online. The PCR products were separated on 1.5% agarose gel by electrophoresis, and sequenced. The sequences were spliced together to obtain full-length cDNA.

Table 1. Relationship between lnc-PKNOX1-1 expression and the clinicopathological features of melanoma patients ($n = 40$)

Characteristics	Number	Expression of lnc-PKNOX1-1		*P* value
		Low	High	
Total cases	40	19	21	
Age (years)				
<60	14	5	9	0.273
≥60	26	14	12	
Sex				
Male	15	7	8	0.935
Female	25	12	13	
Tumor size (cm)				
<4	28	15	13	0.24
≥4	12	4	8	
Ulcer or erosion				
Yes	10	6	4	0.361
No	30	13	17	
Pathological type				
Melanoma *in situ*	12	1	11	**0.001****
Invasive melanoma	28	18	10	
Breslow thickness (mm)				
<1	15	4	11	**0.041***
≥1	25	15	10	
Clark classification				
I–II	22	10	12	0.775
III–V	18	9	9	
TNM stage				
I	21	8	13	0.429
II	15	9	6	
III–IV	4	2	2	
Recurrence or metastasis				
Yes	11	4	7	0.722
No	21	9	12	

**$P < 0.01$ and
*$P < 0.05$ indicate a significant relationship among the variables. Bold values indicate significant *P*-values.

Lnc-PKNOX1-1 identification

The basic characteristics of lnc-PKNOX1-1 were obtained from NONCODE website (www.noncode.org/) and LNCipedia website (www.lncipedia.org/). The genome location was visualized using UCSC genome browser (http://genome.ucsc.edu/) and Illustrator for biological sequences software (http://ibs.biocuckoo.org/) (22). The protein-coding ability of lnc-PKNOX1-1 was predicted by Coding Potential Assessment Tool (CPAT, http://lilab.research.bcm.edu/cpat/) (23), Coding Potential Calculator (CPC2.0, http://cpc2.gao-lab.org/index.php) (24) and LGC algorithm (https://ngdc.cncb.ac.cn/lgc/) (25).

Cytoplasmic and nuclear RNA isolation

Cytoplasmic RNA and nuclear RNA were isolated from A375 and A2058 cells by NE-PER nuclear and cytoplasmic extraction reagents (Thermo Scientific, USA). cDNA was synthesized using RevertAid First Strand cDNA Synthesis Kit (Thermo Scientific, USA), following RT-qPCR using Real-time PCR Master Mix (SYBR Green) 1(TOYOBO, Japan). The primer sequences used are shown in Supplementary Table 1, available at *Carcinogenesis* Online. U6 was used as a nuclear reference, and GAPDH as a cytoplasmic reference. Relative gene expression was calculated using $2^{-\Delta\Delta Ct}$.

RNA fluorescent in situ hybridization assay

RNA fluorescent in situ hybridization (FISH) assay for lnc-PKNOX1-1 was performed using FISH Detection Kit (GenePharma, China) with biotin-labeled LNA probes. The sequences of the lnc-PKNOX1-1 probes are shown in Supplementary Table 1, available at *Carcinogenesis* Online. A375 and A2058 cells were plated on coverslips in 48-well plates and hybridized with biotin-labeled lnc-PKNOX1-1 probes at 37°C overnight. Nuclei were stained using 4′,6-diamidino-2-phenylindole dihydrochloride. Fluorescence was observed under Zeiss LSM800 confocal microscope (Carl Zeiss AG, Germany).

RNA extraction and RT-qPCR

Total RNA was drawn using TRIzol reagent (Invitrogen, USA). Each 1 μg of total RNA was reverse transcribed to 20 μl cDNA using Evo M-MLV RT Mix Kit with gDNA Clean for qPCR (Accurate Biology, China). Then, qPCR was performed with SYBR Green Premix Pro Taq HS qPCR Kit (Accurate Biology, China) and assessed using Light Cycler 480 II Instrument (Roche Applied Science, Germany). The primers of lnc-PKNOX1-1 and GAPDH used are listed in Supplementary Table 1, available at *Carcinogenesis* Online. Relative expression of RNAs was calculated based on $2^{-\Delta\Delta Ct}$.

Protein isolation and western blot analysis

The samples were lysed using RIPA lysis buffer (Beyotime, China) involving phosphatase and protease inhibitors (Roche, Switzerland), and denatured at 100°C for 10 min. Then equal amounts of protein were loaded into 4–20% sodium dodecyl sulfate–polyacrylamide gels. After electrophoresis, the proteins were transferred to polyvinylidene fluoride membranes (Millipore, USA). Non-specific proteins were blocked in EveryBlot Blocking Buffer (Bio-Rad, USA). After incubation in primary antibodies at 4°C overnight, the membranes were incubated with HRP-conjugated anti-rabbit secondary antibody (1:5000; Cell Signaling Technology, USA) at room temperature for 1 h. The protein bands were visualized using enhanced chemiluminescence kit (Beyotime, China). The primary antibodies used are listed in Supplementary Table 2, available at *Carcinogenesis* Online.

Immunofluorescence assay

The cells were cultured in confocal dishes, then fixed and permeabilized. After blocked in 10% goat serum at room temperature for 1 h, the cells were incubated with primary antibodies at 4°C overnight, then incubated in Alexa fluor 647-labeled goat anti-rabbit secondary antibody (1:500, Beyotime, China) in the dark for 1 h. 4′,6-Diamidino-2-phenylindole dihydrochloride was used for nuclear staining. The cells were observed using Olympus IX81 confocal microscope (Olympus, Japan). The primary antibodies used for cell immunofluorescence are listed in Supplementary Table 2, available at *Carcinogenesis* Online.

Cell proliferation assays *in vitro*

For Cell Counting Kit-8 (CCK-8) assay, the cells were planted in 96-well plates at 2 × 10^3 cells per well. CCK-8 dye solution (Dojindo Molecular Technologies, Japan) was added into each well at 24, 48, 72 and 96 h, respectively, then incubated at 37°C for 2 h. Optical density (OD) absorbance value at 450 nm was measured using microplate reader (Thermo Fisher Scientific, USA). For ethynyldeoxyuridine (EdU) assay, the cells were seeded into 96-well plates at 5 × 10^5 cells per well, and incubated with 10 μM EdU at 37°C for 2 h, then fixed and permeated. The cells were dyed with Azide 555 Dye Solution and Hoechst 33342 (Epizyme, China). Three randomly selected fields were photographed under inverted fluorescence microscope. The percentage of EdU-positive cells was calculated as follows: (EdU-positive cells (red dots)/Hoechst-positive cells (blue dots)) × 100%.

Cell migration and invasion assays *in vitro*

For wound-healing assay, the cells were planted in 6-well plates by 5 × 10^5 cells each well. Three straight scratches were drawn in each well using 200 μl pipette-tip, and washed with phosphate-buffered saline. The relative migrating distance was assessed by photos taken at 0 and 48 h using ImageJ. For transwell assay, 24-well plates with permeable membrane inserts of 8-μm pores (Corning Costar, USA) were adopted. Membranes pretreated with Matrigel (BD Biosciences, USA) were used for invasion assay, while membranes without pretreatment were for migration assay. The cells were seeded in upper chambers (5 × 10^4 cells per well) and cultured in fetal bovine serum-free Dulbecco's modified Eagle's medium, then 20% fetal bovine serum-Dulbecco's modified Eagle's medium was added into lower chambers. After 36 h, the cells on membranes were fixed and dyed with 0.1% crystal violet. In each chamber, three fields were randomly photographed under inverted fluorescence microscope. The invaded and migrated cells were counted using ImageJ.

Flow cytometric analysis

The cells were planted in 6-well plates at 8 × 10^5 cells each well. After fixed in 95% ethanol at −20° for 24 h, the cells were treated with Cell Cycle Assay Kit (Fcmacs, China) following the manufacturer's instructions. Then flow cytometric analysis were performed on FACSVerse flow cytometer (BD Biosciences, USA).

In vivo xenograft experiment

Twelve 5-week-old male BALB/c nude mice were randomly divided into two equal groups and kept under pathogen-free conditions. Each mouse was subcutaneously injected with 200 μl cell suspension of 5 × 10^6 A375 vector or OE-PKNOX1-1 cells into the armpit of the right forelimb. Tumor volume was measured twice a week, and calculated by 0.5 × (length × width^2). The mice were euthanized and photographed 28 days after injection. The transplanted tumors were taken out for photographs and weighting. The animals were treated humanely, complying with the National Institutes of Health Guide for the Care and Use of Laboratory Animals. This animal experiment program obtained the consent of the Animal Care and Use Committee of our hospital (approval number: 2021-DW-003).

Protein array analysis

A2058 cells of the control and OE-PKNOX1-1 groups were lysed with lysis buffer involving phosphatase and protease inhibitors (Roche, Switzerland). The lysates were analyzed by human cytokine antibody arrays (G-series 5 [AAH-CYT-G5], RayBiotech, USA). Triplicates were designed for each group. Signals were detected by InnoScan 300 Microarray Scanner (Innopsys, France). The data were analyzed using RayBio AAH-CYT-G5 Analyzer (Raybiotech, USA). Differentially expressed genes (DEGs) were defined as those with fold change greater than 1.5 times (over 1.5-fold or less than 0.67-fold), and P value less than 0.05. Kyoto Encyclopedia of Genes and Genome (KEGG) pathway and Gene Ontology (GO) enrichment analyses were performed using DAVID bioinformatics resources (https://david.ncifcrf.gov/) (26,27). In both analyses, the screening criteria were the number of DEGs of a certain pathway or term ≥4, and $P < 0.05$.

ELISA

The cells were planted at 8 × 10^5 cells per well in 6-well plates, and cultured for 24 h. The culture supernatant was collected to detect the concentration of IL-8 using Human IL-8 Valukine ELISA (Novus Biologicals, USA) following the manufacturer's protocol.

Statistical analysis

All experiments were performed in triplicate and repeated at least three times. The software programs used for statistical analyses were Microsoft Office Excel, IBM SPSS Statistics 26, GraphPad Prism6 and ImageJ. The relationship between lnc-PKNOX1-1 expression and clinicopathological characteristics of melanoma patients was analyzed using the Pearson χ^2 test. Differences between experimental and control groups were determined using the two-tailed Student's t-test. Multiple comparisons were performed using the one- and two-way ANOVA tests. Quantitative data were presented as the mean ± standard deviation (SD). P values of <0.05 were considered statistically significant and were indicated by $^*P < 0.05$, $^{**}P < 0.01$, $^{***}P < 0.001$ and $^{****}P < 0.0001$.

Results

Identification of lnc-PKNOX1-1 in melanoma

In previous study, we found that THOC2 is an oncogene in melanoma progression. Microarray analysis unveiled 877 downregulated genes and 720 upregulated genes in A375 cells after THOC2 knockdown (18). Among the downregulated genes, lnc-PKNOX1-1 was the most significant one. According to NONCODE website, LNCipedia website and UCSC genome browser, lnc-PKNOX1-1 is an intergenic lncRNA encoded on human chromosome 21 (hg38, chr21:42953779–42956378), which consists of two exons (chr21:42953779–42954939 and chr21:42955326–42956378) (Figure 1A). However, its function has not been reported in previous literature.

First 3′ and 5′ RACE assay was performed (Figure 1B) to obtain the full-length sequence of lnc-PKNOX1-1, which was 2212 bp (Supplementary Figure 1A, available at *Carcinogenesis* Online). The sequence of lnc-PKNOX1-1 was also searched on LNCipedia. However, there are subtle differences between the two sequences. The sequence from RACE assay has one base 'G' more at 42955736, one base

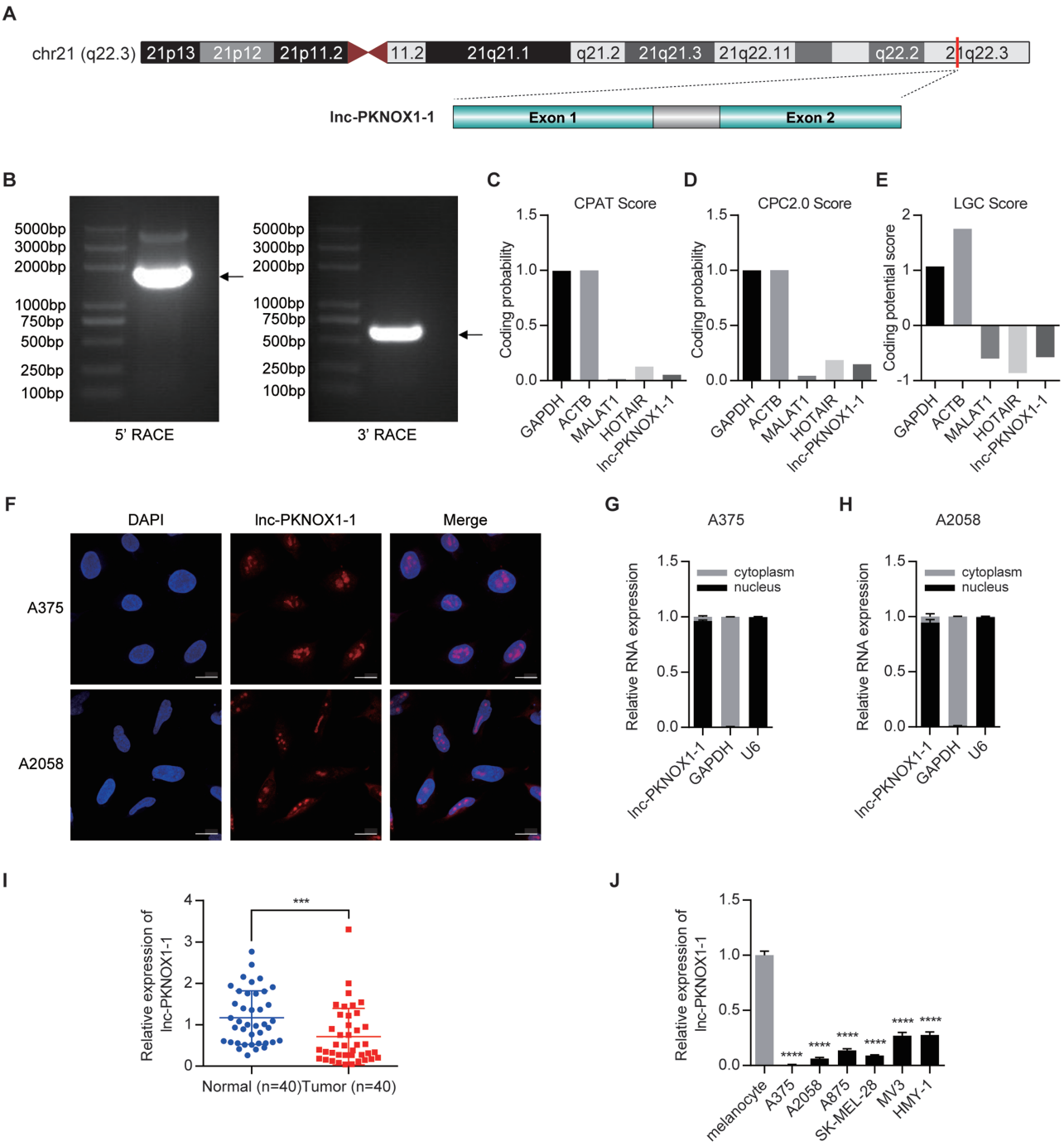

Figure 1. Identification of lnc-PKNOX1-1 and its subcellular localization and expression in melanoma. (**A**) Schematic diagram of the chromosomal location of lnc-PKNOX1-1 in UCSC genome browser, and its composition of two exons visualized by Illustrator for biological sequences software. (**B**) Representative images of lnc-PKNOX1-1 PCR products of the 5′- and 3′-RACE assay on agarose gel. (**C–E**) The protein-coding potential of lnc-PKNOX1-1 predicted through CPAT, CPC2.0 and LGC algorithms, with GAPDH and ACTB being coding RNA controls, and MALAT1 and HOTAIR being non-coding RNA controls. (**F**) FISH assay revealed that lnc-PKNOX1-1 is primarily located in nuclei of A375 and A2058 cells. The nucleus stained with DAPI, lnc-PKNOX1-1 RNA detected by biotin-labeled LNA probes, and the merged images were shown; scale bar = 20 μm. (**G–H**) Cytoplasmic and nuclear RNA isolation followed by RT-qPCR showed lnc-PKNOX1-1 mainly located in the nuclei of A375 and A2058 melanoma cells. GAPDH and U6 were applied as positive controls in the cytoplasm and nucleus, respectively. (**I**) Relative expression of lnc-PKNOX1-1 in forty pairs of melanoma tissues and adjacent normal tissues by RT–qPCR. Bars in the scatterplot show the mean ± SD of each group. (**J**) Relative expression of lnc-PKNOX1-1 in six melanoma cell lines and human primary normal melanocytes by RT–qPCR. Data were analyzed with the two-tailed Student's *t*-test, and presented as the mean ± SD from at least three biological replicates. ***$P < 0.001$ and ****$P < 0.0001$ are the significance levels. DAPI, 4′,6-diamidino-2-phenylindole dihydrochloride.

'G' replaced by 'A' at 42955763 and one base 'G' less at 42956378 than the sequence from LNCipedia.

Then protein-coding potential was predicted. GAPDH and ACTB served as coding RNA controls, while MALAT1 and HOTAIR as non-coding RNA controls. The predicting result of CPAT, CPC2.0 and LGC algorithm all indicated that lnc-PKNOX1-1 lacks the potential to code for human protein (Figure 1C–E).

RNA FISH assay (Figure 1F) as well as cytoplasmic and nuclear RNA isolation assay (Figure 1G and H) were used to

investigate the subcellular localization. Both results showed that lnc-PKNOX1-1 was primarily located in the nuclei of A375 and A2058 cells. Taken together, we proved that lnc-PKNOX1-1 is a nucleus-localized, long non-protein-coding RNA.

Lnc-PKNOX1-1 is downregulated in melanoma tissues and cell lines

To detect the effect of lnc-PKNOX1-1 on melanoma, first we isolated total RNA of forty pairs melanoma tissues and adjacent normal tissues from the patients enrolled. The results of RT-qPCR demonstrated that lnc-PKNOX1-1 was significantly decreased in melanoma tissues than the normal tissues (Figure 1I). We further performed RT-qPCR in human primary normal melanocytes and six human melanoma cell lines, including A375, A2058, A875, SK-MEL-28, MV3 and HMY-1. A significantly lower expression of lnc-PKNOX1-1 was observed in melanoma cell lines than melanocytes (Figure 1J). These results suggested that lnc-PKNOX1-1 might exert tumor-inhibitory effect on melanoma. To understand the clinical significance of lnc-PKNOX1-1 in melanoma, the Pearson χ^2 test was used to analyze the correlation between lnc-PKNOX1-1 expression and the clinicopathological characteristics of the melanoma patients (Table 1). The results suggested that low lnc-PKNOX1-1 expression was significantly associated with invasive pathological type ($P = 0.001$) and Breslow thickness ($P = 0.041$) of melanoma. There was no significant correlation between lnc-PKNOX1-1 expression and age, sex, tumor size, ulcer, Clark classification, TNM stage, recurrence or metastasis (Table 1).

Lnc-PKNOX1-1 inhibits proliferation of melanoma cells

Since lnc-PKNOX1-1 was found low expressed in melanoma, lnc-PKNOX1-1-overexpressed cell lines were constructed in A375 and A2058 cells to find out the function of lnc-PKNOX1-1 in melanoma. The overexpression efficiency was assessed by RT-qPCR (Figure 2A and B), and lnc-PKNOX1-1 expression level was compared among melanocytes and melanoma cells with or without lnc-PKNOX1-1 overexpression (Supplementary Figure 1B, available at *Carcinogenesis* Online). CCK-8 and EdU assays were conducted to examine the function of lnc-PKNOX1-1 in melanoma cell viability and proliferation. CCK-8 assay indicated that lnc-PKNOX1-1 overexpression significantly inhibited melanoma cell proliferation (Figure 2C and D). EdU assay showed that the percentage of EdU-positive cells was lower in OE-PKNOX1-1 group than the control group, suggesting that lnc-PKNOX1-1 decreased melanoma cell proliferation (Figure 2E–H). These results indicated that lnc-PKNOX1-1 might possess a negative function in melanoma cell proliferation.

Lnc-PKNOX1-1 inhibits cell cycle of melanoma cells

As overexpression of lnc-PKNOX1-1 suppressed melanoma cell proliferation, we further explored the influence of lnc-PKNOX1-1 on cell cycle progression. The results of flow cytometric analysis demonstrated that the percentage of A375 and A2058 cells was significantly increased in G0/G1 phase while decreased in S phase after lnc-PKNOX1-1 overexpression (Figure 2I–K). In addition, cell cycle promoting cyclins (Cyclin A2, Cyclin D1 and Cyclin E2), cyclin-dependent kinase 2 (CDK2) and p21 cyclin inhibition protein 1 (p21cip1, hereafter referred to as p21) were detected by western blot (Figure 2L–N). Lnc-PKNOX1-1 overexpression caused a decrease in Cyclin A2, Cyclin D1, Cyclin E2 and CDK2, which are vital proteins for promoting cell cycle transition from G1 to S phase. While lnc-PKNOX1-1 overexpression generated a significant increase in p21, which could lead to cell cycle arrest. The above results suggested that lnc-PKNOX1-1 might regulate the expression of cell cycle-related proteins, thus restricting melanoma cells' entry from G1 into S phase.

Lnc-PKNOX1-1 inhibits migration and invasion of melanoma cells

Metastasis of melanoma is closely correlated with poor prognosis. To explore whether lnc-PKNOX1-1 influenced melanoma migration and invasion, we carried out wound-healing and transwell assays. Wound-healing assay revealed that the healing rate of melanoma cells was reduced by lnc-PKNOX1-1 overexpression, uncovering the role of lnc-PKNOX1-1 in impairing migration ability of melanoma cells (Figure 3A–D). This result was further confirmed by Transwell assay without Matrigel (Figure 3E–H). Matrigel-coated transwell assay showed that lnc-PKNOX1-1 overexpression significantly reduced the number of invaded melanoma cells compared with the control group (Figure 3I–L). These results indicated that lnc-PKNOX1-1 significantly impaired migration and invasion of melanoma cells.

Lnc-PKNOX1-1 inhibits epithelial–mesenchymal transition in melanoma cells

It has been acknowledged that epithelial–mesenchymal transition (EMT) process is highly correlated with tumor metastasis and invasion (28). Therefore, we detected the influence of lnc-PKNOX1-1 on EMT-related proteins in melanoma cells through western blot and cell immunofluorescence assays. We found that after lnc-PKNOX1-1 was overexpressed, mesenchymal cell markers N-cadherin, Vimentin and Snail were downregulated, while epithelial cell marker E-cadherin was upregulated, which indicated that EMT was impaired by lnc-PKNOX1-1 (Figure 3M–O). Cell immunofluorescence assay further confirmed the results (Figure 3P and Q).

Lnc-PKNOX1-1 inhibits tumor growth of melanoma *in vivo*

To verify the impact of lnc-PKNOX1-1 on melanoma progression *in vivo*, we injected A375 cells of OE-PKNOX1-1 group or the control group into nude mice. During the process of xenograft tumor growth, lnc-PKNOX1-1 overexpression led to slower tumor growth than the control group (Figure 4A). Twenty-eight days after injection, xenograft tumors of OE-PKNOX1-1 group were significantly smaller and lighter than those of the control group (Figure 4A–C). The above results confirmed that upregulation of lnc-PKNOX1-1 suppressed melanoma cell proliferation *in vivo*.

Identification of DEGs in microarray and functional enrichment analysis

To gain further insight into how lnc-PKNOX1-1 inhibits melanoma progression, we performed a high-throughput protein microarray analysis in A2058 cells of OE-PKNOX1-1 group and the control group (triplicates of each group). DEGs are

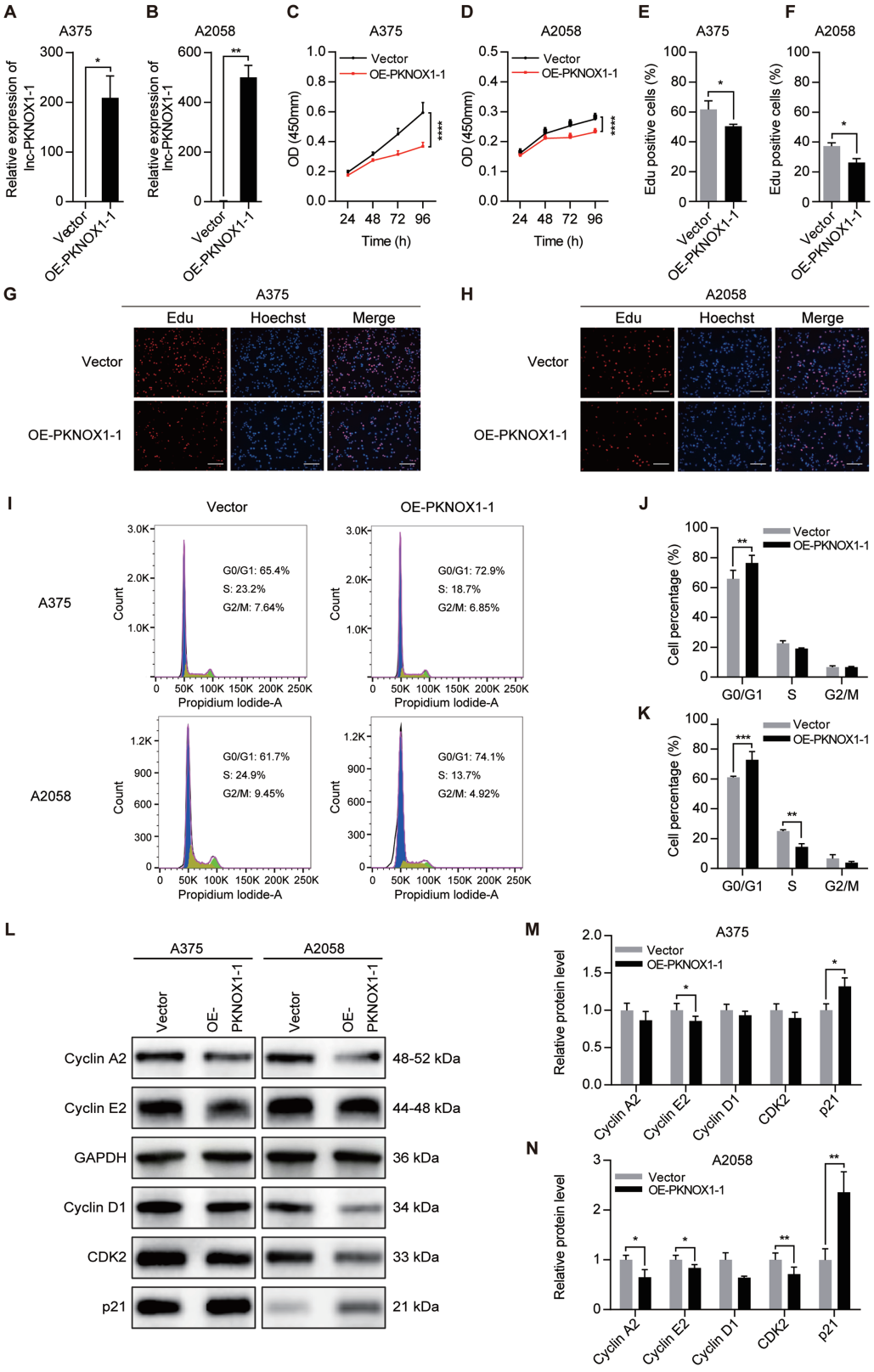

Figure 2. Lnc-PKNOX1-1 suppresses proliferation and cell cycle progression of A375 and A2058 cells. (**A** and **B**) The successful construction of lnc-PKNOX1-1-overexpressed and control A375 and A2058 cell lines were confirmed by RT-qPCR. (**C** and **D**) CCK-8 assay to explore the influence of lnc-PKNOX1-1 on melanoma cell proliferation. (**E**–**H**) EdU assay to evaluate the role of lnc-PKNOX1-1 in melanoma cell proliferation; scale bar = 200 μm. (**I**–**K**) Flow cytometric analysis to explore the impact of lnc-PKNOX1-1 on melanoma cell cycle progression. (**L**–**N**) Western blot assay to explore the impact of lnc-PKNOX1-1 on cell cycle proteins in melanoma cells. The results above were from at least three independent repeats and obtained through analyses performed using the two-tailed Student's *t*-test and two-way ANOVA. Bars indicated the mean ± SD of the triplicates in each condition. $^{*}P < 0.05$, $^{**}P < 0.01$, $^{***}P < 0.001$ and $^{****}P < 0.0001$ indicate the significance levels.

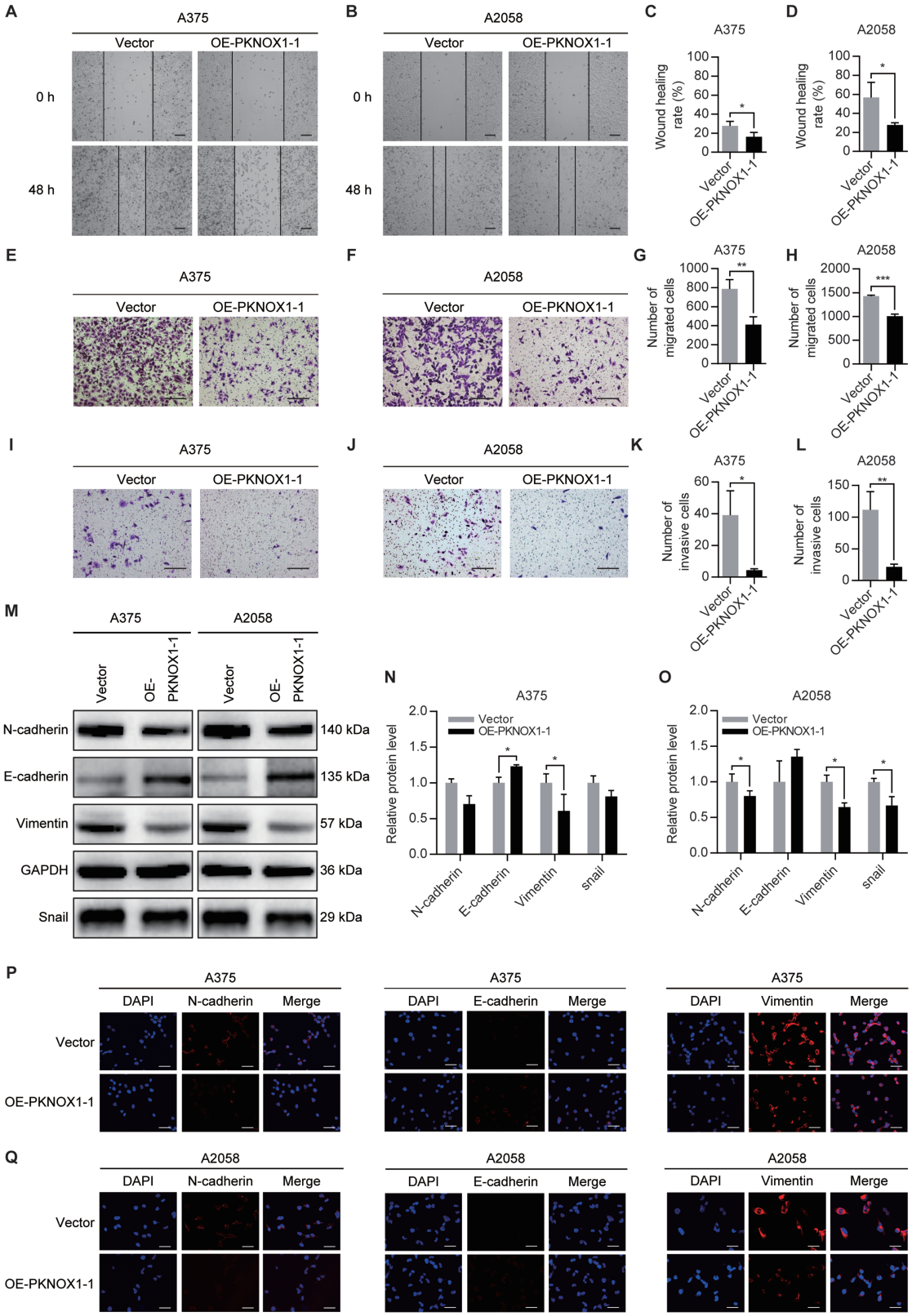

Figure 3. Lnc-PKNOX1-1 inhibits migration, invasion, and EMT of A375 and A2058 cells. (**A**–**D**) Wound-healing assay to explore the role of lnc-PKNOX1-1 in melanoma cells migration; scale bar = 200 μm. (**E**–**H**) Transwell assay without Matrigel to explore the role of lnc-PKNOX1-1 on migration of melanoma cells; scale bar = 100 μm. (**I**–**L**) Matrigel-coated transwell assay to study the impact of lnc-PKNOX1-1 on melanoma cell invasion; scale bar = 100 μm. (**M**–**O**) Western blot assay to explore the impact of lnc-PKNOX1-1 on EMT-related proteins in melanoma cells. (**P** and **Q**) Cell immunofluorescence assay to explore the influence of lnc-PKNOX1-1 on EMT-related proteins in melanoma cells; scale bar = 50 μm. The results above were obtained from at least three independent repeats and analyses were performed using the two-tailed Student's *t*-test. Bars indicate the mean ± SD of the triplicates in each condition. $^{*}P < 0.05$, $^{**}P < 0.01$ and $^{***}P < 0.001$ are the significance levels.

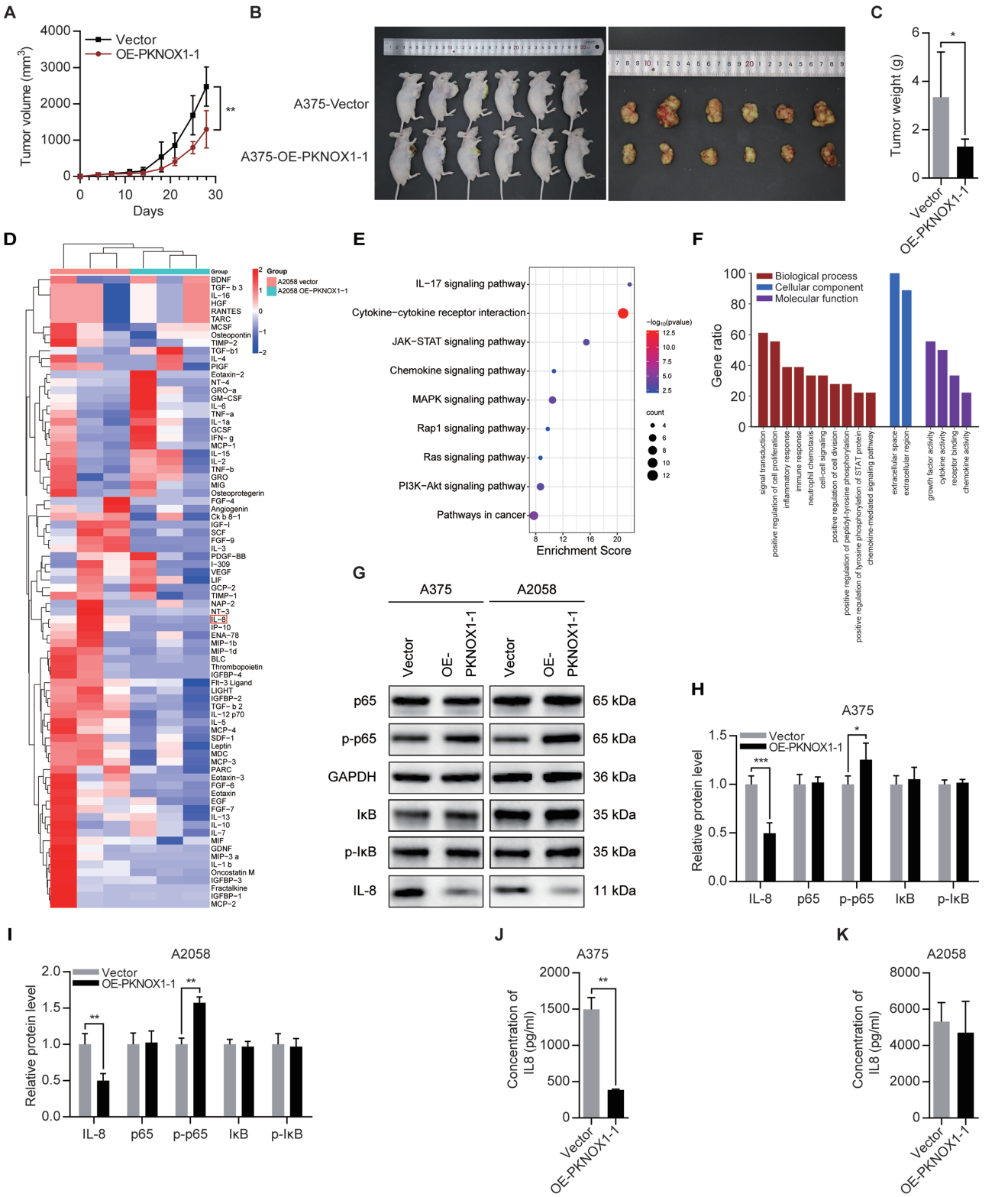

Figure 4. Effect of lnc-PKNOX1-1 on tumor growth of melanoma by *in vivo* assay, and identification of DEGs by microarray analysis, enrichment analysis, western blot and ELISA. (**A**) Tumor volumes were measured twice a week in the mice after being injected with A375 cell suspensions of OE-PKNOX1-1 and control group, and tumor growth curves were drawn. (**B**) The mice were euthanized and photographed 28 days after injection, and the tumors were taken out from the mice for photographs and weighting. (**C**) Tumor weights were measured after tumors were taken out from the mice. (**D**) Heatmap of protein expression in microarray analysis in A2058 cells of OE-PKNOX1-1 group and the control group (triplicates of each group). (Red represents upregulated genes; blue represents downregulated genes; white represents unchanged genes.) (**E**) Some of the significant KEGG pathways ($P < 0.05$) of the DEGs. (**F**) Biological process, cellular component and molecular function ($P < 0.05$) in GO enrichment analysis of the DEGs. (**G**–**I**) Protein expression levels of IL-8, p65, p-p65, IκB and p-IκB in OE-PKNOX1-1 group and the control group of A375 and A2058 cells were measured by western blot; bar charts represent the mean ± SD from three independent experiments. (**J** and **K**) Secreted IL-8 level in OE-PKNOX1-1 group and control group of A375 and A2058 cells was measured by ELISA in triplicate and repeated for three times independently. Data are presented as the mean ± SD. Significant differences were evaluated using the Student's *t*-test and two-way ANOVA, and significant findings were presented as $*P < 0.05$, $**P < 0.01$ and $***P < 0.001$.

defined as those with fold change greater than 1.5 times (over 1.5-fold or less than 0.67-fold), and *P* value less than 0.05. The heatmap of the protein expression is presented in Figure 4D. After lnc-PKNOX1-1 was overexpressed, 18 genes were significantly downregulated in A2058 cells. Detailed information about the 18 DEGs is presented in Supplementary Table 3, available at *Carcinogenesis* Online. KEGG pathway analysis suggested that DEGs were mainly enriched in pathways relevant to inflammatory process and tumorigenesis, such as cytokine–cytokine receptor interaction, chemokine signaling pathway, JAK–STAT signaling pathway (Figure 4E). Moreover, GO enrichment analysis revealed that signal transduction, cell proliferation, inflammatory response and immune response were mostly affected by lnc-PKNOX1-1 (Figure 4F).

Effects of lnc-PKNOX1-1 on IL-8 and nuclear factor-kappa B signaling pathway

From protein microarray analysis, we noticed that IL-8 was significantly downregulated after lnc-PKNOX1-1 overexpression, and enriched in multiple signaling pathways, for instance, cytokine–cytokine receptor interaction, chemokine signaling pathway, IL-17 signaling pathway, etc. Numerous studies have confirmed that IL-8 plays a vital part in melanoma progression and metastasis, and is symbolic for advanced melanoma diagnosis (29,30). We hypothesized that overexpressed lnc-PKNOX1-1 inactivated IL-8 transcription, thus inhibited melanoma progression. To test this hypothesis, we performed western blot and ELISA, and the results showed that IL-8 expression and secretion were significantly reduced in OE-PKNOX1-1 group of A375 and A2058 cells (Figure 4G–K).

IL-8 is a downstream molecule of nuclear factor-kappa B (NF-κB) signaling pathway (31), so western blot was also used to explore the correlation between lnc-PKNOX1-1 and NF-κB signaling pathway in A375 and A2058 cells. The results showed no significant differences in IκB, p-IκB and p65 expression between OE-PKNOX1-1 group and the control group, but p-p65 at Ser536 was significantly upregulated in response to lnc-PKNOX1-1 overexpression (Figure 4G–I). The above results suggested that lnc-PKNOX1-1 upregulation could reduce IL-8 expression and promote p65 phosphorylation at Ser536 in melanoma.

Rescue assay: IL-8 rescues the tumor-suppressing function of lnc-PKNOX1-1 in melanoma cells

To explore whether IL-8 is the functional downstream mediator of lnc-PKNOX1-1-induced tumor inhibition in melanoma, rescue experiments were carried out. Lnc-PKNOX1-1-overexpressed A375 and A2058 cells pretreated with 10 ng/ml IL-8 were OE-PKNOX1-1 + IL-8 groups. CCK-8 and EdU assay proved that viability and proliferation ability of melanoma cells were stronger in OE-PKNOX1-1 + IL-8 group than OE-PKNOX1-1 group (Figure 5A–C and Supplementary Figure 1C and D, available at *Carcinogenesis* Online). In cell cycle assay, we observed that OE-PKNOX1-1 + IL-8 group showed a decreasing percentage of melanoma cells in G0/G1 phase and an increasing percentage of melanoma cells in S phase compared with OE-PKNOX1-1 group (Figure 5D–F). Western blot assay showed that Cyclin D1, Cyclin E2 and CDK2 were upregulated, and p21 was downregulated in OE-PKNOX1-1 + IL-8 group (Supplementary Figure 1E–G, available at *Carcinogenesis* Online). These results suggested that IL-8 might rescue the inhibition of G1 to S phase transition by lnc-PKNOX1-1, therefore promoting melanoma cell cycle progression. Wound-healing and transwell migration assays proved that melanoma cells of OE-PKNOX1-1 + IL-8 group showed higher migration ability compared with OE-PKNOX1-1 group (Figure 5G–I and Supplementary Figure 1H–K, available at *Carcinogenesis* Online). Furthermore, western blot detecting EMT-related proteins showed upregulation of N-cadherin and Vimentin, and downregulation of E-cadherin in OE-PKNOX1-1 + IL-8 group compared with OE-PKNOX1-1 group (Figure 5J–L). All the above results indicated that IL-8 overexpression could partially reverse the inhibition effects of lnc-PKNOX1-1 on melanoma cell proliferation, cell cycle, migration and EMT process.

Discussion

lncRNAs have been proved to participate in numerous cellular processes, and be strictly regulated in physiological conditions as well as multiple diseases (32). LncRNAs in nucleus exert their functions mainly through regulating chromosome structure and function, and *cis-/trans*-regulating gene transcription. LncRNAs in cytoplasm mostly play their roles at post-transcriptional level, such as regulating mRNA translation, degradation and intracellular signaling pathway. LncRNAs in organelles are usually involved in regulating organelle function and metabolism (32). Over the years, studies on lncRNAs have attracted increasing interests, a reason for which is their involvement in tumorigenesis, including melanoma (33,34). For instance, Zhang *et al.* proved that LncRNA HOXD-AS1 promoted melanoma proliferation and invasion (35). Siena *et al.* suggested that lncRNA U731166 was associated with melanoma invasion and vemurafenib resistance (36). Therefore, lncRNAs are promising to become a biomarker or target in melanoma.

In this study, our team identified a new lncRNA in melanoma, lnc-PKNOX1-1, which is an intergenic lncRNA of 2212 bp, mainly located in cell nucleus. Lnc-PKNOX1-1 was found significantly less expressed in CMM tissues than normal tissues, and in human melanoma cells than human primary melanocytes. Besides, low expression of lnc-PKNOX1-1 was proved significantly correlated with higher invasive pathological type and Breslow thickness of melanoma. On this basis, we constructed lnc-PKNOX1-1-overexpressing stable cell lines in A2058 and A375 cells. CCK-8, EdU and nude mice tumor formation assays showed that lnc-PKNOX1-1 significantly suppressed melanoma cell proliferation and viability both *in vitro* and *in vivo*. Flow cytometric and western blot analyses suggested that lnc-PKNOX1-1 could restrict melanoma cell cycle progression. Wound-healing and transwell assays proved that lnc-PKNOX1-1 inhibited melanoma cell migration and invasion. Besides, western blot and immunofluorescence assays proved that EMT of melanoma cells was inhibited by lnc-PKNOX1-1. Therefore, the above data strongly suggested the inhibitory function of lnc-PKNOX1-1 in melanoma. To further detect the mechanism by which lnc-PKNOX1-1 affects melanoma, protein array analysis was performed. IL-8 was found negatively regulated after lnc-PKNOX1-1 overexpression. Western blot

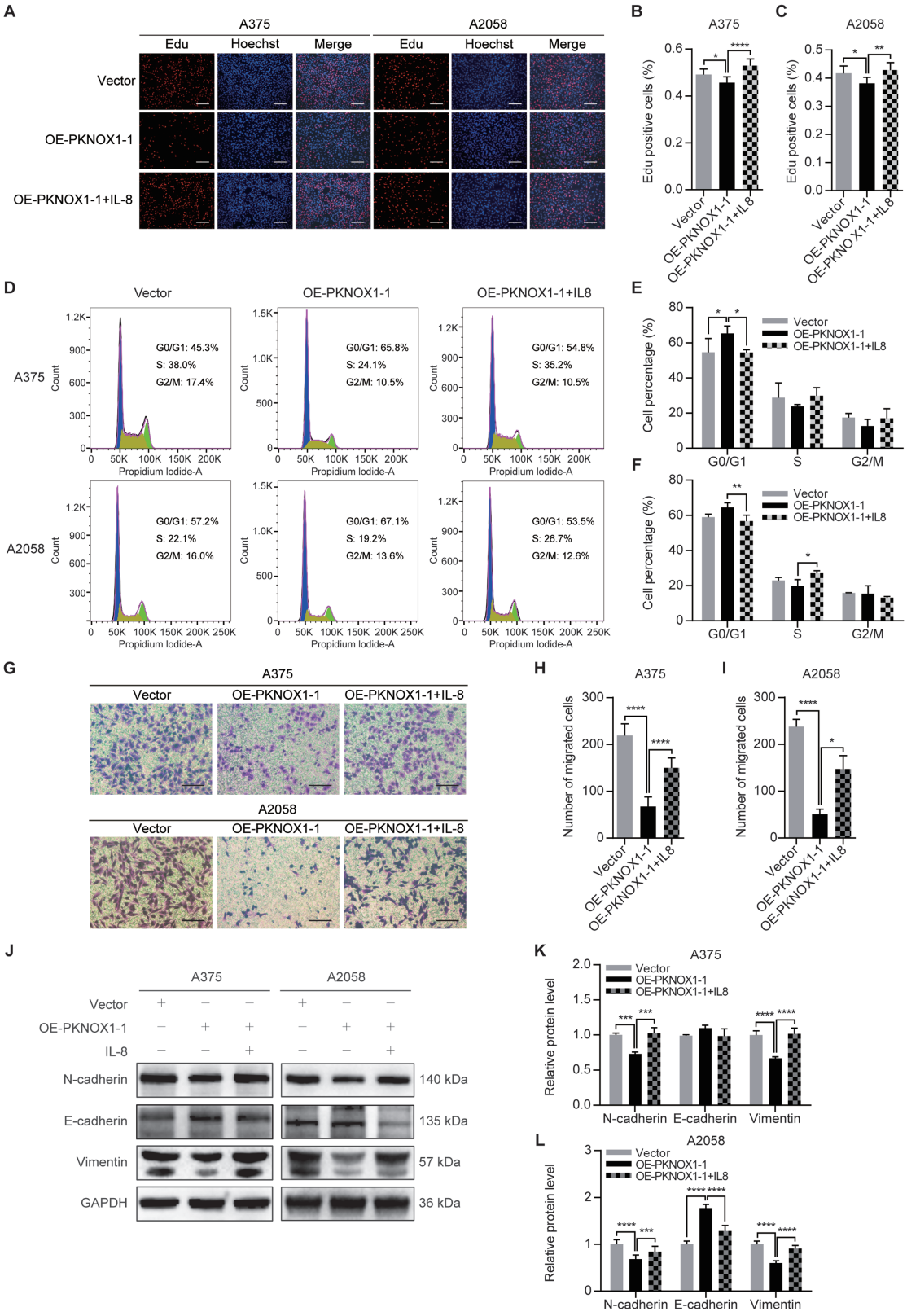

Figure 5. IL-8 rescues the inhibiting function of lnc-PKNOX1-1 on proliferation, cell cycle progression, migration and EMT in melanoma cells. (**A**–**C**) EdU assay to test the impact of IL-8 on melanoma cell proliferation inhibited by lnc-PKNOX1-1. (**D**–**F**) Flow cytometric analysis to explore the impact of IL-8 on cell cycle progression of OE-PKNOX1-1 melanoma cells. (**G**–**I**) Transwell migration assay to test the impact of IL-8 on migration ability of OE-PKNOX1-1 melanoma cells. (**J**–**L**) Western blot to explore the role of IL-8 on EMT-related proteins in OE-PKNOX1-1 melanoma cells. The results above were from at least three independent repeats and were obtained through analyses performed using the one- and two-way ANOVA. Bars indicate the mean ± SD of the triplicates in each condition. *$P < 0.05$, **$P < 0.01$, ***$P < 0.001$ and ****$P < 0.0001$ are the significance levels.

and ELISA analyses further confirmed that IL-8 expression and secretion were reduced by lnc-PKNOX1-1. In addition, KEGG pathway enrichment and GO biological process have shown that lnc-PKNOX1-1 might be involved in immunity, inflammation and tumorigenesis and affect multiple related pathways. Western blot also revealed that in NF-κB signaling pathway, lnc-PKNOX1-1 could promote the phosphorylation of p65 at Ser536 in melanoma. Rescue assays proved that IL-8 overexpression partially reversed the tumor-inhibitory function of lnc-PKNOX1-1 in melanoma cells, implying that lnc-PKNOX1-1 could suppress melanoma development by regulating IL-8.

IL-8 was initially known as a proinflammatory CXC chemokine, guiding neutrophils to the site of infection. Recently, IL-8 has been found associated with tumors. The serum concentration of IL-8 has been proved correlated with tumor burden in multiple tumors, including melanoma (29,37,38). And the rate of IL-8 positivity tends to increase as melanoma stage progresses (38). Moreover, in melanoma patients using immune checkpoint blockade, serum IL-8 level precisely correlates with tumor burden, clinical response and overall survival (39). Therefore, IL-8 is vital for advanced melanoma diagnosis and therapy. NF-κB family is pivotal in regulating inflammation, immune response and cancer (40). Accumulating evidence has indicated the relationship between aberrant activation of NF-κB signaling pathway and cancer progression (41). In addition, it has been proved that IL-8 transcription is regulated by NF-κB signaling pathway (42,43). Multiple studies have confirmed that the site-differential phosphorylation of p65 may exert totally different effects in diverse tumors (44). P65 phosphorylation at Ser536 was reported to drive hepatocellular carcinogenesis (45), while exert inhibitory effect in breast cancer, colorectal cancer, prostatic cancer, etc. (44,46), but its influence on melanoma has not been reported. In this study, lnc-PKNOX1-1 was proved to promote p65 phosphorylation at Ser536, while the expression of IκB, p-IκB and p65 was unaffected. Also, IL-8 was identified as one of the downstream targets of lnc-PKNOX1-1. A hypothetical mechanism might involve that lnc-PKNOX1-1 suppresses IL-8 secretion via regulating p65 phosphorylation in NF-κB signaling pathway, thus modulating melanoma phenotype.

In summary, lnc-PKNOX1-1 is significantly less expressed in melanoma and closely associated with its pathological type and Breslow thickness. Upregulation of lnc-PKNOX1-1 can inhibit various malignant phenotypes of melanoma by inhibiting IL-8 expression. Overall, the results of our work indicated the potential role of lnc-PKNOX1-1 as a valuable prognostic indicator and promising therapeutic target for melanoma patients.

Supplementary material

Supplementary data are available at *Carcinogenesis* online.

Funding

This work was supported by the National Natural Science Foundation of China (81872216) and the National Key Research and Development Program of China (2022YFC2504700, 2022YFC2504701, 2022YFC2504705).

Acknowledgements

We are grateful to Professor Xiulian Xu from Hospital of Dermatology, Chinese Academy of Medical Sciences for offering us A875 and MV3 melanoma cell lines. And we would like to thank Professor Yan Kong from Peking University Cancer Hospital and Institute for sharing HMY- 1 melanoma cell line with us.

Conflict of Interest Statement

All authors declared that they have no conflict of interests.

Ethical approval

The studies involving human participants were approved by Ethics Committee of the Institute of Dermatology, Chinese Academy of Medical Sciences and Peking Union Medical College. The patients/participants provided their written informed consent to participate in this study. The animal study was approved by Ethics Committee of the Institute of Dermatology, Chinese Academy of Medical Sciences and Peking Union Medical College.

Authors' contributions

A.L.H., Y.W. and T.L. conceived and designed the experiments. A.L.H., M.C. and Y.X.W. performed the experiments and did data analysis. Y.W. and D.Q.L. provided technical support and critical comments. A.L.H. drafted the manuscript. Y.W., G.Q.Z., F.F., L.Z. and Q.W. provided clinical resources of the patients. Y.W. provided funding support. All authors participated in the revision of the manuscript and approved the submitted version.

Data availability

The data underlying this article will be shared on reasonable request to the corresponding author.

References

1. Grafanaki, K. *et al.* (2023) Noncoding RNA circuitry in melanoma onset, plasticity, and therapeutic response. *Pharmacol. Ther.*, 248, 108466.
2. Brunsgaard, E.K. *et al.* (2023) Melanoma in skin of color: Part I. Epidemiology and clinical presentation. *J. Am. Acad. Dermatol.*, 89, 445–456.
3. Long, G.V. *et al.* (2023) Cutaneous melanoma. *Lancet*, 402, 485–502.
4. Castro-Pérez, E. *et al.* (2023) Connecting the dots: melanoma cell of origin, tumor cell plasticity, trans-differentiation, and drug resistance. *Pigment Cell Melanoma Res.*, 36, 330–347.
5. Fujimura, T. *et al.* (2022) Immunotherapy for melanoma: the significance of immune checkpoint inhibitors for the treatment of advanced melanoma. *Int. J. Mol. Sci.*, 23, 15720.
6. Li, L. *et al.* (2021) Noncoding RNAs: emerging players in skin cancers pathogenesis. *Am. J. Cancer Res.*, 11, 5591–5608.
7. Kopp, F. *et al.* (2018) Functional classification and experimental dissection of long noncoding RNAs. *Cell*, 172, 393–407.
8. Xiao, B. *et al.* (2021) Identification of epithelial–mesenchymal transition-related prognostic lncRNAs biomarkers associated with melanoma microenvironment. *Front. Cell Dev. Biol.*, 9, 679133.
9. Wang, J. *et al.* (2020) LncRNA HOTAIR promotes proliferation of malignant melanoma cells through NF-κB pathway. *Iran. J. Public Health*, 49, 1931–1939.

10. Wang, P. *et al*. (2020) LncRNA MALAT1 promotes the proliferation, migration, and invasion of melanoma cells by downregulating miR-23a. *Cancer Manag. Res*., 12, 6553–6562.
11. Han, X. *et al*. (2021) lncRNA TINCR attenuates the proliferation and invasion, and enhances the apoptosis of cutaneous malignant melanoma cells by regulating the miR-424-5p/LATS1 axis. *Oncol. Rep*., 46, 238.
12. Zhou, X. *et al*. (2019) Long noncoding RNA CPS1-IT1 suppresses melanoma cell metastasis through inhibiting Cyr61 via competitively binding to BRG1. *J. Cell. Physiol*., 234, 22017–22027.
13. Yang, X. *et al*. (2020) Long non-coding RNA GAS5 in human cancer. *Oncol. Lett*., 20, 2587–2594.
14. Hussen, B. *et al*. (2021) Role of lncRNA BANCR in human cancers: an updated review. *Front. Cell Dev. Biol*., 9, 689992.
15. Melixetian, M. *et al*. (2022) Regulation of LncRNAs in melanoma and their functional roles in the metastatic process. *Cells*, 11, 577.
16. Cantile, M. *et al*. (2017) HOTAIR role in melanoma progression and its identification in the blood of patients with advanced disease. *J. Cell. Physiol*., 232, 3422–3432.
17. De Falco, V. *et al*. (2021) Comprehensive review on the clinical relevance of long non-coding RNAs in cutaneous melanoma. *Int. J. Mol. Sci*., 22, 1166.
18. Zhou, X. *et al*. (2019) Knockdown THOC2 suppresses the proliferation and invasion of melanoma. *Bioengineered*, 10, 635–645.
19. Fu, S. *et al*. (2018) Inhibition of interleukin 8/C-X-C chemokine receptor 1,/2 signaling reduces malignant features in human pancreatic cancer cells. *Int. J. Oncol*., 53, 349–357.
20. Rankin, L. *et al*. (2020) Relative deficiency of anti-inflammatory N-acylethanolamines compared to prostaglandins in oral lichen planus. *Biomedicines*, 8, 481.
21. Yamanaka, T. *et al*. (2020) Nintedanib inhibits intrahepatic cholangiocarcinoma aggressiveness via suppression of cytokines extracted from activated cancer-associated fibroblasts. *Br. J. Cancer*, 122, 986–994.
22. Liu, W. *et al*. (2015) IBS: an illustrator for the presentation and visualization of biological sequences. *Bioinformatics*, 31, 3359–3361.
23. Wang, L. *et al*. (2013) CPAT: Coding-Potential Assessment Tool using an alignment-free logistic regression model. *Nucleic Acids Res*., 41, e74.
24. Kang, Y.J. *et al*. (2017) CPC2: a fast and accurate coding potential calculator based on sequence intrinsic features. *Nucleic Acids Res*., 45, W12–W16.
25. Wang, G. *et al*. (2019) Characterization and identification of long non-coding RNAs based on feature relationship. *Bioinformatics*, 35, 2949–2956.
26. Huang da, W. *et al*. (2009) Systematic and integrative analysis of large gene lists using DAVID bioinformatics resources. *Nat. Protoc*., 4, 44–57.
27. Sherman, B.T. *et al*. (2022) DAVID: a web server for functional enrichment analysis and functional annotation of gene lists (2021 update). *Nucleic Acids Res*., 50, W216–W221.
28. Tang, Y. *et al*. (2020) EMT-inducing transcription factors, drivers of melanoma phenotype switching, and resistance to treatment. *Cancers (Basel)*, 12, 2154.
29. Filimon, A. *et al*. (2021) Interleukin-8 in melanoma pathogenesis, prognosis and therapy—an integrated view into other neoplasms and chemokine networks. *Cells*, 11, 120.
30. Timani, K.A. *et al*. (2018) Tip110/SART3 regulates IL-8 expression and predicts the clinical outcomes in melanoma. *Mol. Cancer*, 17, 124.
31. Hoffmann, E. *et al*. (2002) Multiple control of interleukin-8 gene expression. *J. Leukoc. Biol*., 72, 847–855.
32. Statello, L. *et al*. (2021) Gene regulation by long non-coding RNAs and its biological functions. *Nat. Rev. Mol. Cell Biol*., 22, 96–118.
33. Beermann, J. *et al*. (2016) Non-coding RNAs in development and disease: background, mechanisms, and therapeutic approaches. *Physiol. Rev*., 96, 1297–1325.
34. Liu, S.J. *et al*. (2021) Long noncoding RNAs in cancer metastasis. *Nat. Rev. Cancer*, 21, 446–460.
35. Zhang, H. *et al*. (2017) LncRNA HOXD-AS1 promotes melanoma cell proliferation and invasion by suppressing RUNX3 expression. *Am. J. Cancer Res*., 7, 2526–2535.
36. Siena, A.D.D. *et al*. (2022) Upregulation of the novel lncRNA U731166 is associated with migration, invasion and vemurafenib resistance in melanoma. *J. Cell. Mol. Med*., 26, 671–683.
37. Alfaro, C. *et al*. (2017) Interleukin-8 in cancer pathogenesis, treatment and follow-up. *Cancer Treat. Rev*., 60, 24–31.
38. Katoh, Y. *et al*. (2022) Combination of serum 5-S-cysteinyldopa, melanoma inhibitory activity and IL-8 improves the diagnostic accuracy of malignant melanoma compared with individual markers. *Medicine (Baltim.)*, 101, e30471.
39. Sanmamed, M. *et al*. (2017) Changes in serum interleukin-8 (IL-8) levels reflect and predict response to anti-PD-1 treatment in melanoma and non-small-cell lung cancer patients. *Ann. Oncol*., 28, 1988–1995.
40. Mitchell, S. *et al*. (2016) Signaling via the NFkappaB system. *Wiley Interdiscip. Rev. Syst. Biol. Med*., 8, 227–241.
41. Hoesel, B. *et al*. (2013) The complexity of NF-κB signaling in inflammation and cancer. *Mol. Cancer*, 12, 86.
42. Yi, T. *et al*. (2019) Activation of lncRNA lnc-SLC4A1-1 induced by H3K27 acetylation promotes the development of breast cancer via activating CXCL8 and NF-kB pathway. *Artif. Cells Nanomed. Biotechnol*., 47, 3765–3773.
43. Collins, T. *et al*. (2000) Paclitaxel up-regulates interleukin-8 synthesis in human lung carcinoma through an NF-kappaB- and AP-1-dependent mechanism. *Cancer Immunol. Immunother*., 49, 78–84.
44. Bu, Y. *et al*. (2016) A phosphomimetic mutant of RelA/p65 at Ser536 induces apoptosis and senescence: an implication for tumor-suppressive role of Ser536 phosphorylation. *Int. J. Cancer*, 138, 1186–1198.
45. Xu, X. *et al*. (2021) Phosphorylation of NF-kappaBp65 drives inflammation-mediated hepatocellular carcinogenesis and is a novel therapeutic target. *J. Exp. Clin. Cancer Res*., 40, 253.
46. Bu, Y. *et al*. (2016) Targeting NF-kappaB RelA/p65 phosphorylation overcomes RITA resistance. *Cancer Lett*., 383, 261–271.